Original research article

International Journal of ENGINE RESEARCH

International J of Engine Research
1–15

DOI: 10.1177/14680874261441707
journals.sagepub.com/home/jer
Sage

Active pre-chamber ignition with supplemental air scavenging on a two-stroke UAV engine using gasoline and heavy fuels

Daniel Nicklowitz[1], Harold Schock[1,2], Fawaz Imtiaz[1], Alex Szumko[1], Sean Hilbert[3], Thomas Stuecken[1], Jeff Chockley[3], Jennifer Higel[2] and Jim Newton[3]

Abstract

An active pre-chamber ignition system with supplemental scavenge air, delivered via a poppet valve, has been implemented on a small-bore two-stroke engine for drone applications. The engine was operated either using the pre-chamber ignition mode or the standard spark ignition mode by swapping the cylinder head. Multiple fuels were examined, including pre-mixed gasoline and two kerosene-based military fuels with varying cetane ratings (30 and 50). During the pre-chamber tests, the fueling in the crankcase was reduced and instead delivered via the pre-chamber to reduce fuel short-circuiting. Fuel economy and emissions characteristics were assessed for both pre-chamber and traditional spark ignition modes. The results comparing the two ignition systems operating on gasoline revealed a 39.7% decrease in specific fuel consumption at low-speed conditions and a 30.9% decrease at cruising speed, while also reducing hydrocarbon emissions by up to 50%. When operating on the kerosene-based fuels, the pre-chamber ignition mode yielded up to a 44.6% decrease and 29.7% decrease in indicated specific fuel consumption at the low speed and cruising speed conditions, respectively. These results provide a foundation for future performance mapping and optimization of air-scavenged pre-chamber ignition systems for two-stroke applications. This study addresses a gap in the literature concerning the experimental application of active pre-chamber ignition systems in small-bore two-stroke engines. The system under study mitigates the limitations of passive concepts through active air and fuel scavenging of the pre-chamber.

Keywords

active pre-chamber ignition, pre-chamber scavenging, turbulent jet ignition, Jetfire TJI, two-stroke engines, fuel short-circuiting, drone propulsion, unmanned aerial systems, heavy fuel, JP-5/JP-8

Received: 23 November 2025; accepted: 16 March 2026

Introduction

Two-stroke engines are recognized for their relative simplicity and power density, but have become much less common today due to their generally high fuel consumption and emissions characteristics. Despite their drawbacks, two-stroke engines are still widely used today in unmanned aerial systems (UAS) applications, where weight and power density drive the choice of propulsion system. In a typical crankcase scavenged configuration, the charge is prepared within the crankcase and is then introduced to the combustion chamber via transfer ports in the cylinder liner. An exhaust port is uncovered during the blowdown phase of the expansion stroke to remove combustion products. Because both the transfer port and exhaust port are open simultaneously, a significant fraction of the fresh charge delivered via the transfer port is lost through the exhaust port

[1]Michigan State University, East Lansing, MI, USA
[2]Mid-Michigan Research LLC, Brighton, MI, USA
[3]Cobra AERO LLC, Hillsdale, MI, USA

Corresponding author:
Daniel Nicklowitz, Energy and Automotive Research Laboratory, Michigan State University, 426 Auditorium Rd, East Lansing, MI 48824, USA.
Email: nicklow1@msu.edu

during scavenging. This is referred to as short-circuiting when the intake charge contains fuel. As much as 40%–50% of the intake charge may pass directly out of the exhaust port without participating in combustion.[1,2]

Short-circuiting can be minimized, and scavenging improved by optimizing the exhaust geometry to yield the desired wave dynamics and flow characteristics. This works well over a somewhat narrow range of operating conditions, that is, engine speeds, but is difficult to achieve across the entire operating range. Therefore, scavenging is typically poor at low engine speeds, leaving a high residual fraction within the cylinder after the gas exchange procedure. This can lead to high cycle-to-cycle variability, misfires, and generally poor performance at low engine speeds.[3]

Direct injection has been implemented to reduce fuel short-circuiting losses, as the fuel can be delivered late in the scavenging process, separately from the air entering via the transfer port. Several researchers have demonstrated very significant improvements in specific fuel consumption and corresponding reductions in hydrocarbon emissions.[4–6] Direct injection systems are generally classified as low-pressure direct injection (LPDI), with injection pressure of approximately 5 bar,[5] or high-pressure (HPDI, GDI), with injection pressures ranging from about 50 to 200 bar.[6–8] Low-pressure systems are less complex, although they often yield a slight reduction in peak power compared to crankcase injection, resulting from insufficient atomization under high-load, high-speed conditions.[4,5] High-pressure direct injection enables very late injection with sufficient atomization at the expense of requiring a high-pressure fueling system, which presents unique packaging and weight challenges with respect to small UAV applications.

Mixture injection, where a fuel-air mixture is directly injected into the cylinder, has been applied to two-stroke engines to resolve the atomization issues associated with late fuel injection under low injection pressure.[1,8–11] Among the most successful commercial implementations of mixture injection in two-stroke engines is the air-assisted direct injection (AADI) system developed by Orbital.[12] An example of this system was presented by Worth et al. for a two-stroke marine outboard application.[9] The AADI system consists of two injectors per cylinder, including a conventional low-pressure fuel injector and a direct in-cylinder air-fuel mixture injector. The shearing and expansion of the air-fuel mixture upon injection provide a very finely atomized fuel spray at very low pressure, compared to single-fluid systems using high-pressure direct injection. The AADI system implemented on the Mercury Optimax outboard marine engine used an air pressure of 550 kPa, with a fuel pressure of 620 kPa.[9]

To simplify logistics and promote the safe transport of fuel, the US military requires UAS power plants to operate on kerosene-based "heavy" fuels (such as JP-5, JP-8, and Jet-A1) in alignment with the "single fuel strategy" proposed in 1988.[13] Spark ignition (SI) of heavy fuel is challenging due to its poor atomization characteristics and knock propensity because of its low octane number. The orbital AADI system has evolved for application within the UAS industry to address the atomization challenge with several examples successfully operating on heavy fuel.[11] When operating on heavy fuel, a slight reduction in peak power compared to gasoline operation is often observed because of knock under high-load operation.[11,14,15]

Increasing the ignition energy is a strategy to promote complete combustion of low-volatility fuels or highly dilute mixtures.[16–19] Pre-chamber ignition systems are one such concept, where ignition first occurs in a small combustion volume within the cylinder head (typically $< 15\%$ of the clearance volume). Combustion within the pre-chamber produces turbulent ignition jets through several connecting orifices, subsequently igniting the bulk charge in the main chamber. Pre-chamber systems are referred to as *active* if they contain a fuel injector within the pre-chamber, and *passive* if the pre-chamber fuel is delivered from the main chamber through the nozzle orifices.

Several studies have found that pre-chamber systems can promote reliable, rapid ignition of kerosene-based mixtures.[15,20–23] Furthermore, pre-chamber systems have been shown to suppress knocking combustion due to the rapid burn rate, thereby reducing the time for end-gas auto-ignition.[15,21–25] For example, Cui et al.[21] studied the combustion and knocking characteristics in a four-stroke Rotax-914 piston aircraft engine fueled with RP-3 aviation kerosene, equipped with a passive pre-chamber and an air-assisted direct injection system. The knock-limited IMEP could be extended by 13.9%–31.9% over the SI ignition mode, depending on the operating condition. Under low speed and throttled operation, the pre-chamber exhibited slower heat release than SI due to exhaust residuals remaining inside the pre-chamber from the previous cycle. The reduced turbulent kinetic energy within both chambers under throttled conditions was determined to influence the scavenging of exhaust residuals within the pre-chamber. Other researchers have noted the influence of exhaust residuals within the pre-chamber, irrespective of the main chamber dilution rate.[26] Additionally, the authors noted overheating issues with the larger, better-performing pre-chamber. These issues are addressed within this study.

Wang et al. compared the combustion characteristics of gasoline to RP-3 aviation kerosene in a Rotax-914 piston engine.[15] Compared to gasoline, they found the kerosene-based fuel exhibited a long ignition delay and 21.2% longer combustion duration. A passive pre-chamber jet ignition (PJI) system was implemented, which accelerated the burn duration to be equivalent to that of gasoline operated in an SI configuration. The effect of the PJI system compared to SI on knocking combustion was assessed using RP-3, where a 10% to 27% increase in knock-limited IMEP using PJI was observed at different operating conditions.

While the previously mentioned studies were carried out on four-stroke architectures, the literature on pre-chamber-initiated combustion in small two-stroke engines is very limited, and nearly nonexistent for systems operating on heavy fuel. Bosi et al. compared a passive pre-chamber ignition system to SI on a gasoline-fueled 50 cc two-stroke engine with an LPDI injection system.[27] Two pre-chambers were tested, one with six 1 mm orifices and one with six 1.5 mm orifices. Both pre-chambers significantly accelerated the burn rate and improved the combustion stability over SI, although the 1.5 mm orifice configuration offered superior performance compared to the 1 mm orifice across the operating range. Beyond 7500 rpm, stable combustion was not achieved using either pre-chamber configuration. This was attributed to insufficient time for fuel atomization and transfer across the pre-chamber orifices. Bosi later presented another performance comparison of SI versus several different passive pre-chamber geometries at three operating conditions in a 49.2 cc two-stroke engine.[28] The optimal pre-chamber geometry was dependent on the operating conditions, and the pre-chamber ignition strategy yielded higher brake efficiency at mid-load, mid-speed, and wide-open-throttle conditions. At low speed and load, combustion was unstable using the pre-chamber system. This was attributed to the high amount of residual gas within the pre-chamber at this operating condition. An external pre-chamber scavenging system, such as an air injector, was proposed to enhance combustion stability.

From these studies, it can be concluded that there are barriers to implementing passive pre-chamber systems on small-bore two-stroke engines due to their inability to provide reliable ignition across all operating conditions. At low speeds and loads, insufficient scavenging of the pre-chamber leads to unstable combustion. At wide open throttle, there may be insufficient time for fuel atomization and transfer through the passive pre-chamber orifices. Resolving these issues would enable the implementation of pre-chamber combustion systems on small two-stroke engines and the exploitation of their benefits, particularly in terms of power density, burn duration, and knock suppression.

This study presents the application of an active pre-chamber ignition concept with supplemental air scavenging to a small-bore two-stroke engine, addressing these challenges. By implementing a supplemental pre-chamber scavenging system, the exhaust residuals are effectively purged from the pre-chamber under all operating conditions. Coupling the supplemental air scavenging with an active pre-chamber system (containing a fuel injector) allows for precise mixture control within the pre-chamber. The pre-chamber system under discussion is referred to as Jetfire®, and is further described below.

Introduction to Jetfire®

Jetfire® is an active Turbulent Jet Ignition (TJI) system with supplemental air scavenging. Compressed air and fuel are delivered to the pre-chamber shortly before ignition, enabling precise control of the mixture quality. This level of mixture control promotes reliable ignition where traditional TJI systems are likely to struggle, such as under highly dilute main chamber conditions. Compressed air is delivered through a cam-actuated poppet valve. For the four-stroke application, a high-pressure direct injector is located within the pre-chamber. A low-pressure injector is placed upstream of the poppet valve in the two-stroke system, as described in more detail in the following section. An example of the in-cylinder pre-chamber and main chamber pressure traces from a two-stroke operating cycle is shown in Figure 1. The small difference between the pre-chamber and main chamber pressure is a result of the large orifice area to pre-chamber volume ratio, which was chosen to enable the bulk charge to be delivered through the pre-chamber injector. Some key geometric pre-chamber parameters are provided in Table 1.

The system has been extensively studied for four-stroke engine applications operating with high rates of cooled Exhaust Gas Recirculation (EGR).[29–33] Intake manifold EGR dilution rates up to 50% have been demonstrated,[29] and indicated thermal efficiencies up to 45%. Heavy-fueled operation for two fuels with

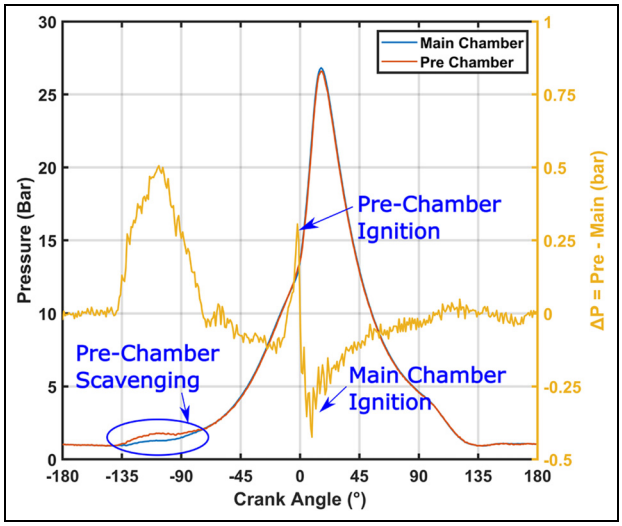

Figure 1. In-cylinder pressure traces and pressure difference.

Table 1. Engine and pre-chamber specifications.

Parameter	Value
Bore	39 mm
Displacement	33.8 cc/cylinder
Geometric compression ratio	8:1
Trapped compression ratio	5:1
Pre-chamber volume	0.67 cc
Pre-chamber orifice	6 mm × 1.5 mm
Injection pressure	3 bar gage
Cooling method	Liquid cooled
Fuel type	Gasoline or heavy fuel (JP-8)

Figure 2. Pre-chamber integrated cylinder head (top view).

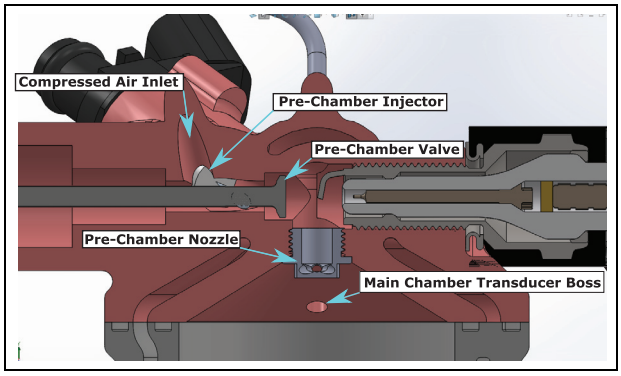

Figure 3. Cross section of pre-chamber head.

varying cetane numbers has also been demonstrated on a four-stroke platform.[22] Given the ability to operate reliably on heavy fuel and under high main chamber dilution rates, the air scavenged pre-chamber system was thought to offer several benefits for two-stroke applications, including:

- Increased burn rate and improved combustion stability across a range of fuels.
- Increased power density due to improved combustion efficiency and the slight supercharging effect of the pre-chamber scavenge air delivery, especially under low to mid speed conditions.
- Reduce or eliminate short circuiting losses under part load, cruising conditions by delivering all fuel through the pre-chamber.
- Increase knock tolerance due to reduced burn duration and improved control over the ignition process, further enabling load extension or an increased compression ratio.

A multi-fuel-capable two-stroke engine for drone applications was modified and instrumented to test these hypotheses. The test bench will now be described in further detail.

Experimental setup

A Cobra Aero A99HF engine platform was configured and instrumented at the Michigan State University Energy and Automotive Research Lab. The engine implements a liquid-cooled, three-cylinder, two-stroke architecture with a displacement of 101.4 cc. The A99HF produces 7 kW at 8500 rpm, and is compatible with gasoline and kerosene-based heavy fuels (JP5, JP8, Jet A) without hardware modification.[34,35] The engine is crankcase-injected, with each cylinder having an independent crankcase. The cylinder heads, engine block, and crankcase are additively manufactured using powder bed fusion, enabling component geometries that would not be feasible using traditional manufacturing methods. This approach also facilitated the production of a prototype cylinder head with an integrated pre-chamber. The pre-chamber volume is 670 mm^3, which is approximately 13.9% of the TDC clearance volume. General engine specifications are provided in Table 1.

The prototype cylinder head, henceforth referred to as the Jetfire head, houses several accessories supporting the pre-chamber scavenging and data acquisition, including a poppet valve for delivering the fresh pre-chamber mixture, a low-pressure fuel injector, a spark plug containing an integrated pre-chamber pressure transducer, a compressed air delivery passage, and a boss for a main chamber pressure transducer. A water jacket cools the cylinder head and pre-chamber assembly. Fuel is injected upstream of the pre-chamber poppet valve. This injector location was chosen primarily to enable a smaller pre-chamber volume as compared to placing the injector directly within the pre-chamber. Figure 2 shows a top view of the prototype cylinder head. Figure 3 shows a rendering of the cylinder head and pre-chamber cross section.

A performance comparison between TJI and SI, based on in-cylinder pressure data, was performed by swapping between the standard and Jetfire cylinder heads. Only one of the three cylinders (cylinder 3) was modified for this experiment, while the other two cylinders used standard heads configured for SI. By comparing the two ignition modes on the same cylinder, the results were not influenced by variations between cylinders. When operating on the Jetfire head, an auxiliary belt-driven camshaft actuated the pre-chamber poppet valve. The camshaft was removed when

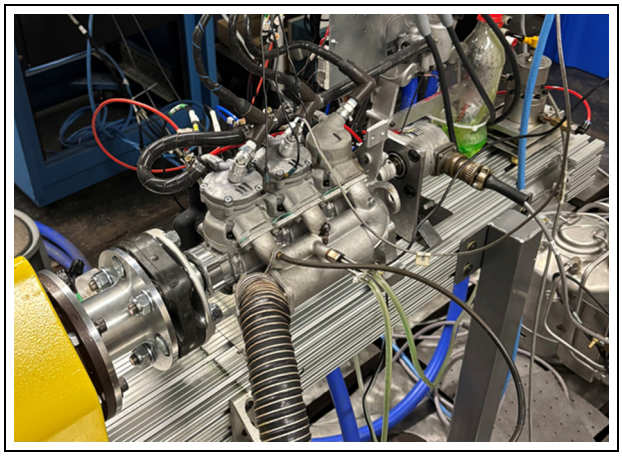

Figure 4. Test stand using standard head.

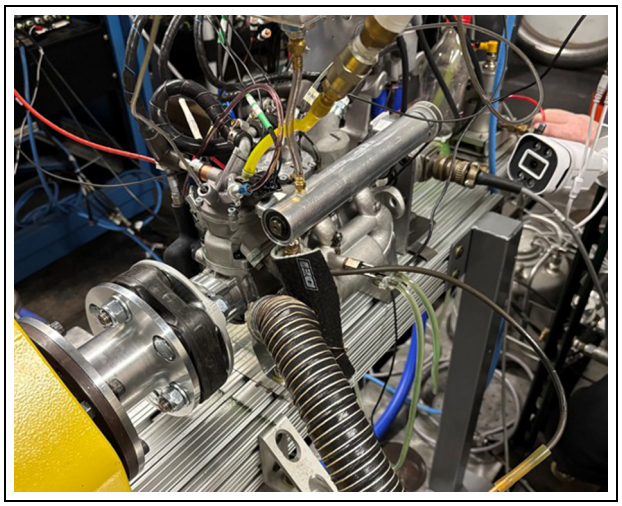

Figure 5. Test stand using jetfire head (with auxiliary camshaft).

operating with the standard SI cylinder head. Figure 4 shows the engine test stand when operating on the standard head, while Figure 5 shows the test bench when operated using the Jetfire head and auxiliary camshaft. Compressed pre-chamber scavenging air was delivered at pressures up to 25 psi gage (PSIg) using the test facility machine shop air compressor. The energy losses associated with compressed air delivery were estimated using equation (5), which was then used to correct the reported engine load and specific fuel consumption.

In-cylinder pressure data were acquired using Kistler piezoelectric pressure transducers, coupled to an A&D charge amplifier and Phoenix CAS combustion analysis system. Jetfire main chamber pressure data were acquired using a Kistler 6054C transducer, and pre-chamber pressure data using a Kistler 6113B spark plug integrated transducer. When testing the standard cylinder head, the 6113B spark plug integrated transducer monitored the main chamber pressure. An optical encoder with a resolution of 1 crank angle degree monitored the crank angle position. A Kistler 4075A

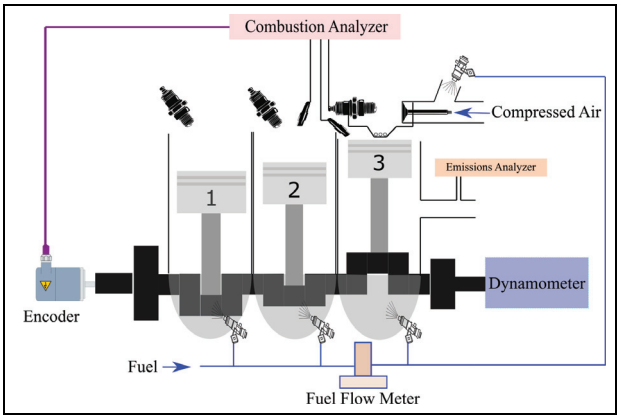

Figure 6. Schematic of test bench configured with the pre-chamber.

piezoresistive pressure transducer was positioned within the cylinder 3 intake runner, and a Kulite EWCT-11-312M water-cooled piezoresistive transducer within the exhaust runner. The fuel flow rate was monitored using a MAX Machinery P001A piston flow meter. Only the fuel flow to cylinder 3 was routed through the fuel flow meter, including both the main chamber and pre-chamber injectors when operated in the TJI mode. Emissions data, including CO, CO2, NO, and hydrocarbon emissions, were monitored using a Horiba MEXA 584L exhaust gas analyzer, where the exhaust gas sampling location was positioned within the cylinder 3 exhaust runner. Pre-chamber scavenge air flow rates were measured using an Omega FMA-1611A flow element. An external 12 V DC source supplied power to the engine ECUs, fuel pump, an electric coolant pump, and several of the instruments mentioned above. The engine was coupled to an AC dynamometer, which was configured to maintain the engine speed at a constant set point, with a maximum speed capability of 6150 rpm. A schematic of the test bench configured with the Jetfire cylinder head is shown in Figure 6.

Combustion analysis parameters

As only a single cylinder was modified for these experiments, the performance of the two ignition modes was assessed based on the in-cylinder pressure data. The *indicated mean effective pressure* (IMEP) is the pressure-volume work developed over the cycle, normalized by the swept volume, as defined in equation (1).

$$IMEP = \frac{1}{V_d}\int pdV \tag{1}$$

Where p and V are the crank angle resolved in-cylinder pressure and volume, respectively, and V_d is the swept volume. The IMEP reported during this work represents the average over 200 cycles for each operating condition. The IMEP is a normalized measure of the engine load, from which the indicated power and

indicated specific fuel consumption (ISFC) can be computed according to equations (2) and (3), where N is the engine speed, and $\dot{m}_{fuel}$ is the fuel mass flow rate.

$$\dot{W}_{ind} = (IMEP) \cdot V_d \cdot N \quad (2)$$

$$ISFC = \frac{\dot{m}_{fuel}}{\dot{W}_{ind}} \quad (3)$$

Combustion stability has been assessed based on the IMEP *coefficient of variation* (COV %), as defined in equation (4). An IMEP COV of less than 5% indicates good combustion stability, while a COV greater than 10% may suggest misfires, partial burns, and overall high cycle-to-cycle variability.

$$IMEPCOV(\%) = \frac{\sigma_{\mathrm{IMEP}}}{\mu_{\mathrm{IMEP}}} \cdot 100\% \quad (4)$$

Where σ_{IMEP} is the standard deviation of the IMEP and μ_{IMEP} is the mean of the IMEP. The COV reported during this work is calculated using the mean and standard deviation of a 200-cycle data set corresponding to each operating condition.

Delivering the scavenge air to the pre-chamber results in a parasitic loss, which has been estimated using the first law approach presented in equation (5).

$$\dot{W}_c = \frac{\dot{m}_{air} \cdot (h_2 - h_1)}{\eta_c} \quad (5)$$

Where $\dot{m}_{air}$ is the pre-chamber scavenge air mass flow rate, h_1 and h_2 are the enthalpies of the air before and after compression, respectively, and η_c is the assumed isentropic compressor efficiency. An isentropic compressor efficiency of $\eta_c = 0.6$ was assumed as a conservative estimate. Air was modeled as an ideal gas, from which the temperature after compression was estimated using polytropic relations with a polytropic exponent of $n = 1.4$. Ideal gas tables were used to interpolate the difference in enthalpy at the two respective states.[36] When reporting measured quantities for the Jetfire head, the parasitic energy loss from pre-chamber scavenging has been subtracted from the IMEP; therefore is also accounted for in the corresponding ISFC.

A relation for the in-cylinder *net rate of heat release*, shown in equation (6), can be derived from a first law analysis by assuming the cylinder consists of a single phase obeying ideal gas relations.[3,37]

$$\frac{dQ_{\mathrm{net}}}{d\theta} = \frac{\gamma}{\gamma - 1} p \frac{dV}{d\theta} + \frac{1}{\gamma - 1} V \frac{dp}{d\theta} \quad (6)$$

Where $\gamma = \frac{c_p}{c_v}$ is the ratio of specific heats, θ is the crank angle. This equation is integrated to arrive at the *cumulative net heat release*.

Testing procedure

Three fuels were examined during this work, including ethanol-free gasoline and two kerosene-based heavy fuels with varying cetane numbers. The low cetane heavy fuel had a cetane number of 30, while the higher cetane fuel had a cetane number of 51. These are referred to as CN30 and CN50, respectively. The engine platform under study does not employ a dedicated separate lubrication system. All lubrication of load-bearing components (e.g. piston, rings, and bearings) is provided solely by two-stroke oil pre-mixed with the fuel. All fuels were pre-mixed with two-stroke oil at a 50:1 ratio by volume. Relevant fuel properties for the kerosene-based fuels are provided in Table 2. The exact properties of the commercial gasoline used in this study were not measured; therefore, representative literature values are reported.

Table 2. Fuel properties.

Property	CN50	CN30	Gasoline[38,39]
Cetane/octane	51 CN	30 CN	91 AKI
Lower heating value (MJ/kg)	43.6	43.6	$\sim$ 43
Density (g/cc)	0.788	0.785	$\sim$ 0.75
Viscosity (cSt)	4.04	4.01	$\sim$ 0.7
Stoichiometric AFR	14.74	14.70	$\sim$ 14.7
Flash point (°F)	122	125.6	< -40

Two operating conditions were selected for this initial study: a low-speed, moderate-load condition of 3 bar IMEP, 3000 rpm, and a cruising-speed, load condition of 4 bar IMEP, 5000 rpm. Each fuel was examined using both ignition modes at these two operating conditions.

A primary motivation of this study was to assess the lowest specific fuel consumption achievable with the two ignition systems at the target operating conditions described above. The following testing methodology was developed to minimize fuel consumption at the target conditions. Using the standard head, the engine was initially operated at a load slightly higher than the target IMEP. The fueling was then reduced until crossing over the target IMEP. This process was repeated for several fixed throttle positions to determine the most optimal SFC at the target load. The ignition timing was continuously adjusted for maximum IMEP.

For the Jetfire ignition tests, the engine was generally operated at a fixed throttle position determined from the SI experiments, and the pre-chamber air pressure was swept instead (up to 25 psi gage). This was done to avoid a very large test matrix and to study the influence of pre-chamber scavenge air pressure on the TJI system performance. Again, the initial fueling was set such that the load slightly exceeded the target IMEP. The fueling was then gradually reduced until crossing over the target. When operating with the Jetfire cylinder head, the main chamber (crankcase) fueling was progressively reduced, and the pre-chamber fueling increased as needed to maintain the target load. At the lowest flow rates, the fuel was entirely delivered via the pre-chamber with no crankcase fueling. This was done to reduce the short-circuiting of fuel during

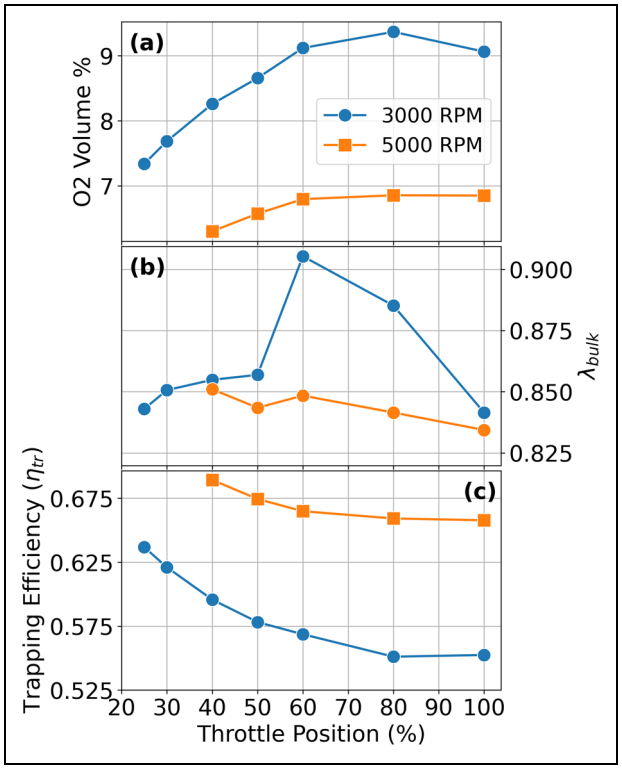

Figure 7. Measure O2 % (a), bulk λ (b), and calculated trapping efficiency (c) at 3000 and 5000 rpm versus throttle position.

the main chamber scavenging process and to evaluate the feasibility of pre-chamber-only fueling as an alternative to other two-stroke direct injection strategies. The engine was only operated in this mode briefly (up to about 1 min per test point) due to the lack of main end bearing lubrication when fueling solely through the pre-chamber.

Estimating the trapping efficiency and trapped air-fuel ratio

Since the intake and exhaust ports are open simultaneously, a significant fraction of the fresh charge is short-circuited during scavenging. The trapping efficiency is defined as the mass ratio of the fresh charge that is trapped to the fresh charge delivered according to equation (7).

$$\eta_{tr} = \frac{m_{\text{air, trapped}}}{m_{\text{air, delivered}}} \tag{7}$$

When operating rich, a simple estimate of the trapping efficiency can be obtained from the exhaust oxygen concentration as shown in equation (8).

$$\eta_{tr} \approx 1 - \frac{[O_2]_{exh}}{[O_2]_{atm}} \tag{8}$$

The portable exhaust gas analyzer available for the main experiments was not equipped with O_2 sampling, so additional experiments were performed to measure the exhaust oxygen concentration at various operating conditions. A Horiba MEXA 7200 exhaust gas analyzer was implemented for these experiments. The engine was operated rich at either 3000 or 5000 rpm and several throttle positions. Figure 7 presents the main result of these experiments, including the O_2 percentage, bulk relative air fuel ratio, and calculated trapping efficiency.

Under rich conditions, the air-fuel ratio (AFR) can be approximated using CO, CO_2, and NO exhaust concentrations according to equation 9.[40]

$$AFR \approx K_f \frac{\frac{1}{2}[CO] + [CO_2] + \frac{1}{4}K_w x([CO] + [CO_2]) + \frac{1}{2}[NO]}{[CO] + [CO_2]} \tag{9}$$

Where x is the fuel hydrogen to carbon ratio, $K_f = 138.18/(12.011 + 1.008x)$, and $K_w = \frac{3.5[CO_2]}{[CO] + 3.5[CO_2]}$. The trapped air mass for each speed, fuel, and throttle position was estimated for the SI ignition mode using the measured fuel flow rate, equation (9) under rich conditions, and the trapping efficiency shown in Figure 7. The trapped air mass was calculated for each fuel, engine speed, and throttle position. The trapped air mass, trapping efficiency, and fuel flow rate were then used to estimate the air-fuel ratio under lean conditions.

When estimating the trapped AFR using the TJI system, the additional scavenge air was added to the trapped air mass used in the SI case. A trapped efficiency of 95% was calculated for the pre-chamber injected mass (fuel + air), which was also verified using a 3-D CONVERGE model of the TJI system. The AFR reported throughout this work is computed according to the total trapped air and fuel. This does not account for the variations between the pre-chamber and main chamber mixture composition. The pre-chamber mixture composition is difficult to isolate from the main chamber composition, although CONVERGE results indicate it to be slightly richer than the main-chamber bulk mixture. Initial CFD modeling results suggest the pre-chamber operated at roughly 0.2 lower relative air-fuel ratio than the main chamber.

Results and discussion

Gasoline results

Figure 8 presents the result of the fuel sweeps near the low-speed target condition operated on gasoline. The IMEP and SFC of the TJI data have been adjusted to account for the estimated pre-chamber air delivery parasitic loss according to equation (5). Several throttle positions are shown to illustrate the test methodology for determining the optimal SFC using each ignition mode. At this operating condition, the lowest SFC while maintaining the 3 bar load target was achieved at 40% throttle using the SI ignition mode, and 50% throttle using the Jetfire TJI ignition strategy. The

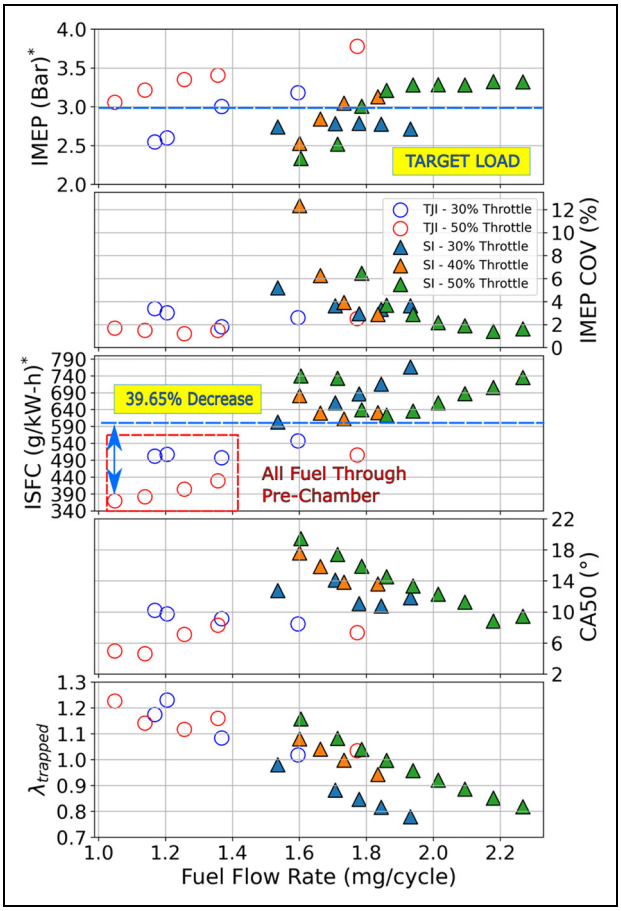

Figure 8. IMEP, COV, ISFC, CA50, and trapped lambda using gasoline with 3000 rpm, 3 bar target.
*IMEP and ISFC corrected for pre-chamber parasitic loss.

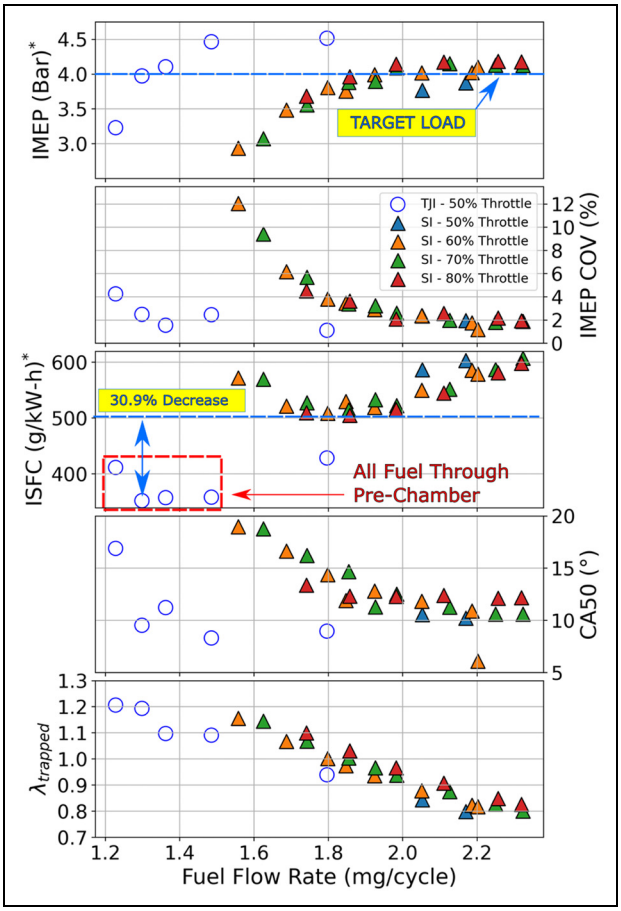

Figure 9. IMEP, COV, ISFC, CA50, and trapped lambda using gasoline with 5000 rpm, 4 bar target.
*IMEP and ISFC corrected for pre-chamber parasitic loss.

3-bar target load could not be maintained with throttle positions below 30%. As the main chamber fueling was reduced, the pre-chamber fueling was increased to maintain the target load with the TJI ignition mode. Fuel was only delivered via the pre-chamber injector for flow rates less than 1.5 $\frac{mg}{cycle}$. A 39.65% reduction in fuel consumption was observed using TJI with all fuel delivered through the pre-chamber compared to the standard SI ignition strategy at 3 bar IMEP and 3000 rpm with gasoline fuel. The TJI system maintained stable combustion at the lowest fuel flow rate tested, with a COV of 1.68% at the most efficient operating point. The SI system combustion stability deteriorated with fuel flow rates below 1.75 $\frac{mg}{cycle}$. Still, the SI exhibited a good COV of 3.93% at the most efficient operating condition. It is essential to note that the SI ignition mode utilized only the crankcase injector; therefore, it was subject to higher short-circuiting losses. While this is an advantage of delivering fuel via the pre-chamber with the TJI system, an equivalent comparison with an LPDI system was not performed during this study. The trapped air fuel ratio result of Figure 8 suggests the TJI system was operated under a slightly leaner bulk in-cylinder mixture composition than the SI system after accounting for the short-circuited fuel, which was up to 42.5% at this operating condition and throttle position according to Figure 7. The variations in AFR during the TJI tests are a result of difficulty in holding the pre-chamber air pressure constant.

Figure 9 shows the comparison of the two ignition modes at 5000 rpm, and nominally 4 bar IMEP operated on gasoline. This operating point was selected to represent cruising conditions in a typical UAV application. Again, several throttle positions are shown for the SI test data, while only a fixed throttle position of 50% was tested for the TJI data at this operating condition with gasoline. At cruising conditions while operating on gasoline, the TJI system exhibited a 30.9% improvement in fuel consumption over the SI system. Again, the fueling was only delivered via the pre-chamber at this flow rate. As with the low speed operating point, combustion became unstable using the SI system for fuel flow rates below 1.75 $\frac{mg}{cycle}$. The Jetfire system maintained stable combustion down to a flow rate of roughly 1.25 $\frac{mg}{cycle}$. The two systems were operated with similar combustion phasing (CA50) during this test, and the trapped AFR estimate suggests the two systems were operated with similar trapped in-cylinder mixture compositions at the lowest fuel flow rates. At a given

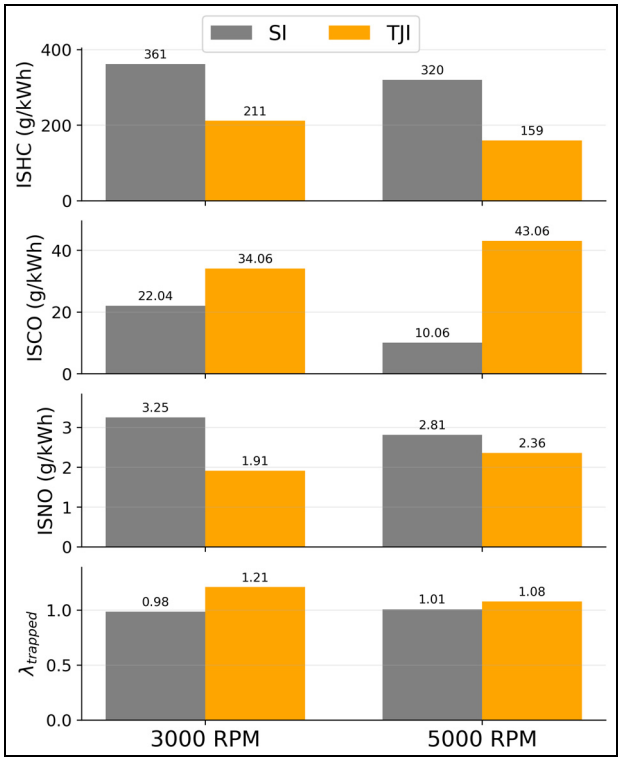

Figure 10. SI versus TJI gasoline emissions.

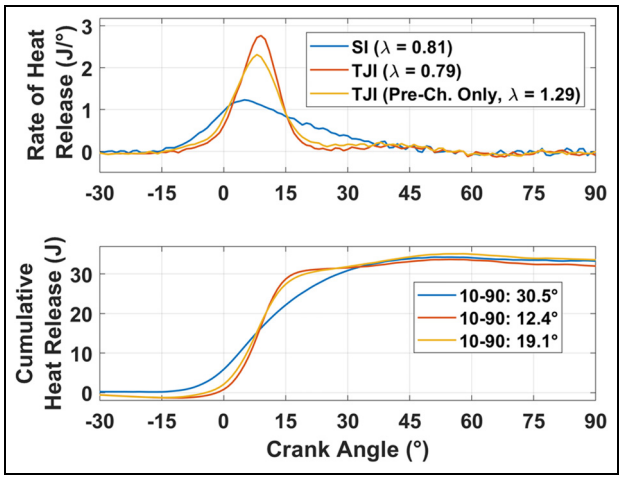

Figure 11. Net rate of heat release and cumulative heat release at 5000 rpm, 4 bar IMEP operated on gasoline.

trapped air-fuel ratio, the TJI system exhibited better combustion stability than the SI system. These results demonstrate that significant improvements in fuel economy can be achieved while maintaining good combustion stability using the TJI fueling and ignition strategy. If a DI system could achieve comparable fuel atomization and burn rates in this small-bore engine, it may also deliver similar fuel economy benefits.

Figure 10 shows the indicated specific emissions measured at both target conditions using gasoline near the minimum SFC observed using each ignition mode. The TJI system exhibits a significant reduction in

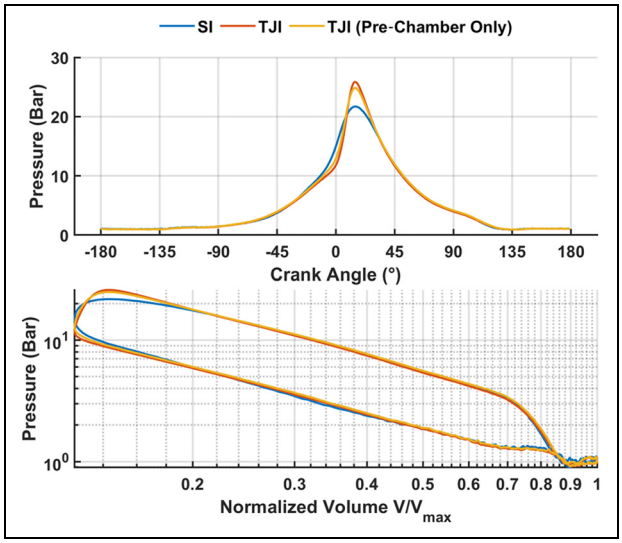

Figure 12. In-cylinder pressure and LogP–LogV diagram at 5000 rpm, 4 bar IMEP operated on gasoline.

hydrocarbon and nitrogen oxide emissions at both operating conditions, although with an increase in *CO*. The decrease in hydrocarbon emissions is primarily driven by the reduced fuel short-circuiting. The pre-chamber fueling strategy may be associated with a charge-cooling effect, which could explain the reduction in *ISNO*. Additionally, the reduced time for fuel evaporation when fueling through the pre-chamber likely explains the increase in *ISCO*.

Figure 11 shows the rate of heat release and the cumulative heat release at cruising conditions for the SI ignition mode, the TJI system operated with main chamber and pre-chamber fueling, and the TJI system operated with only pre-chamber fueling. The 10–90 burn durations are provided in the legend of the cumulative heat release plot. Compared to SI, the TJI ignition strategy yields roughly twice the maximum rate of heat release (ROHR) and up to a 59% faster 10–90 burn duration when operated at a similar trapped air-fuel ratio. A slightly lower maximum ROHR and a small increase in burn duration were observed when fueling only via the pre-chamber as compared to fueling both the main and pre-chamber, although the trapped air-fuel ratio was leaner when fueling only through the pre-chamber injector, which likely influenced the burn rate. Both fueling strategies led to significantly faster combustion using the TJI ignition method when compared to SI. This result demonstrates the benefit of the Jetfire TJI system from a combustion duration perspective. Figure 12 shows the in-cylinder pressure traces and LogP–LogV diagram corresponding to the heat release plots shown in Figure 11. When operating on the TJI system, the bulk charge is consumed rapidly after TDC, resulting in a faster rate of pressure rise and a higher peak cylinder pressure compared to SI. This increases the pressure-volume work developed during the early stage of expansion as shown in the LogP–LogV result

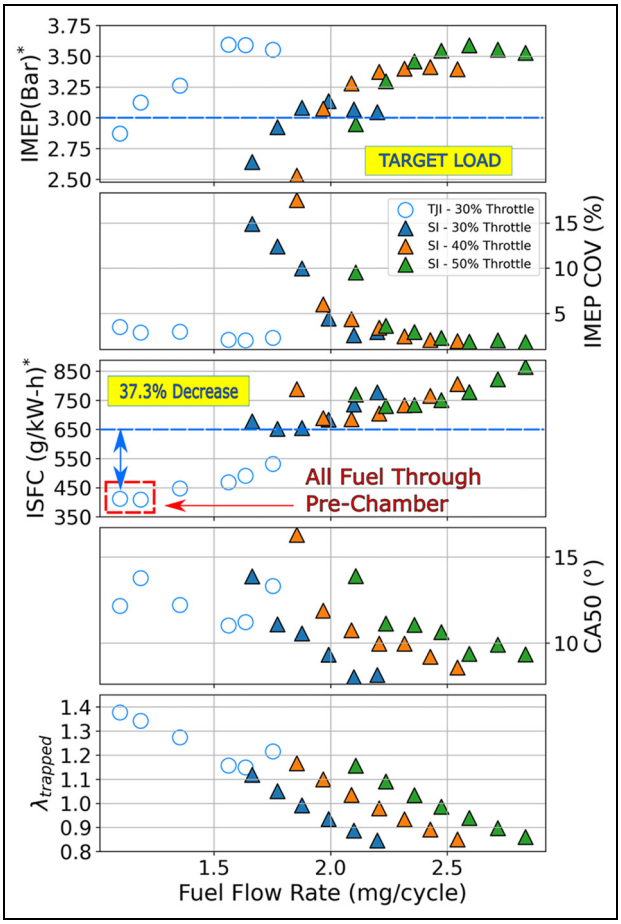

Figure 13. IMEP, COV, ISFC, CA50, and trapped lambda using CN30 fuel with 3000 rpm, 3 bar target.
*IMEP and ISFC corrected for pre-chamber parasitic loss.

of Figure 12. The SI case required earlier ignition timing than the TJI cases to compensate for slower flame propagation, resulting in a modestly higher cylinder pressure late in the compression stroke. Delaying the ignition advance also allows more time for fuel evaporation, which is likely beneficial when adopting the pre-chamber-only fueling strategy due to the later injection timing and shorter fuel flow path compared to crankcase injection.[27]

Heavy fuel results

Following the gasoline experiments, two kerosene-based fuels with varying cetane numbers were examined under equivalent operating conditions using the SI and TJI ignition strategies. As in the previous section, the performance of the two fuels was assessed based on specific fuel consumption, combustion stability, and burn duration. The results of the heavy-fueled experiments are presented in this section.

Figure 13 presents the comparison of the SI and TJI ignition systems operating on the CN30 (low cetane) heavy fuel at nominally 3000 rpm, 3 bar IMEP. The lowest SFC using SI with CN30 fuel was achieved at 30% throttle, while the TJI system was also operated at 30% throttle for this test. At this operating condition, the TJI system achieved a 37.3% reduction over the SI system while fueling entirely through the pre-chamber, as well as a significant improvement in combustion stability. At the lowest SFC, the SI system was operated near the combustion stability limit with a COV of 12.4% at 2.93 bar IMEP. The Jetfire TJI system maintained good combustion stability with a COV of 3.5% at 2.87 bar IMEP after correcting for the parasitic pre-chamber scavenging loss, which resulted in roughly a 0.1 bar reduction at this operating condition. The two ignition systems were operated with similar combustion phasing during these experiments. The trapped air fuel ratio estimate suggests the TJI system was operated roughly 0.3 relative AFR leaner than the SI system at their lowest respective ISFC. This supports the claim that the air-scavenged TJI system can promote reliable ignition of low volatility fuels and dilute mixtures, but should be verified via direct measurement of the air-fuel ratio in the future. The poor combustion stability of the heavy fuel using SI at low speed and low load conditions may be attributed to the lower reactivity and longer ignition delay associated with the fuel, combined with a higher residual mass fraction within the cylinder due to incomplete scavenging at this operating condition. The TJI system overcomes these challenges by distributing ignition sites throughout the main chamber.

Results at 5000 rpm using CN30 fuel are presented in Figure 14. Similar to the results at the low-speed condition, the SI system achieved the best SFC for the target load at a fueling rate near the combustion stability limit, while the TJI system, operating at the same throttle condition, appears to maintain stability for fuel flow rates and loads below the 4 bar target. This suggests that the practical fuel economy benefit of the TJI over SI may be greater than what is suggested by this test strategy, as fueling in practice must be some margin above the stability limit to ensure reliability. The two systems were operated with similar combustion phasing, and the TJI system was operated with a leaner trapped AFR than SI at their most efficient points. At the 4 bar IMEP target and again while fueled entirely via the pre-chamber, the TJI system achieved a 28.5% reduction in fuel consumption over SI at 5000 rpm on the CN30 fuel in this experiment.

The results for the higher cetane fuel (CN50) at the low speed target are presented in Figure 15, while the results for the cruising speed target are presented in Figure 16. At the low-speed operating condition, the trapped air-fuel ratio estimate suggests the TJI system was operated significantly leaner than the SI system at their lowest respective SFC. This operating condition was where the largest percentage improvement in fuel consumption was observed. The TJI system achieved a 44.6% reduction over the SI system when operating on CN50 fuel at 3000 rpm and 3 bar IMEP. This also supports the hypothesis that Jetfire can maintain good

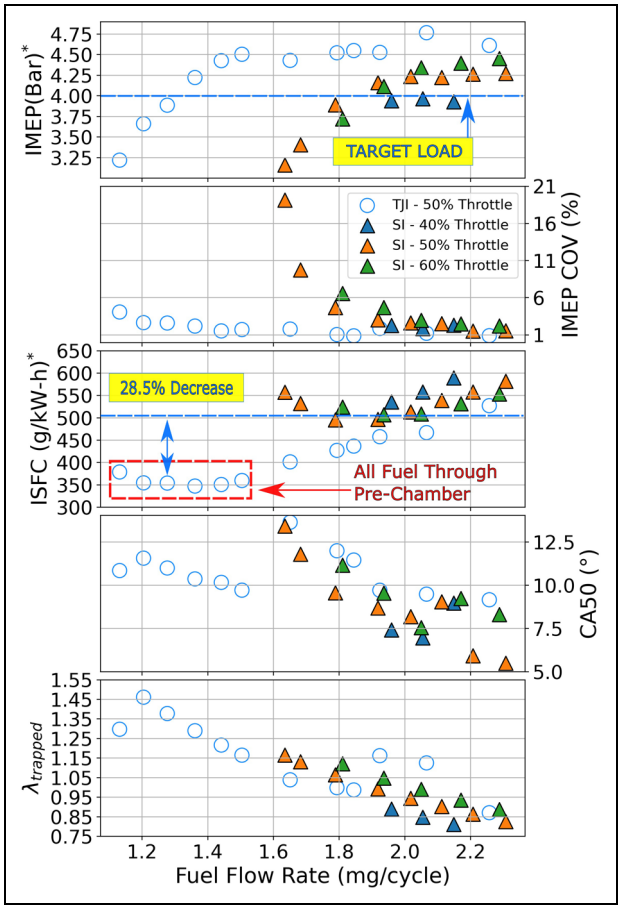

Figure 14. IMEP, COV, ISFC, CA50, and trapped lambda using CN30 fuel with 5000 rpm, 4 bar target.
*IMEP and ISFC corrected for pre-chamber parasitic loss.

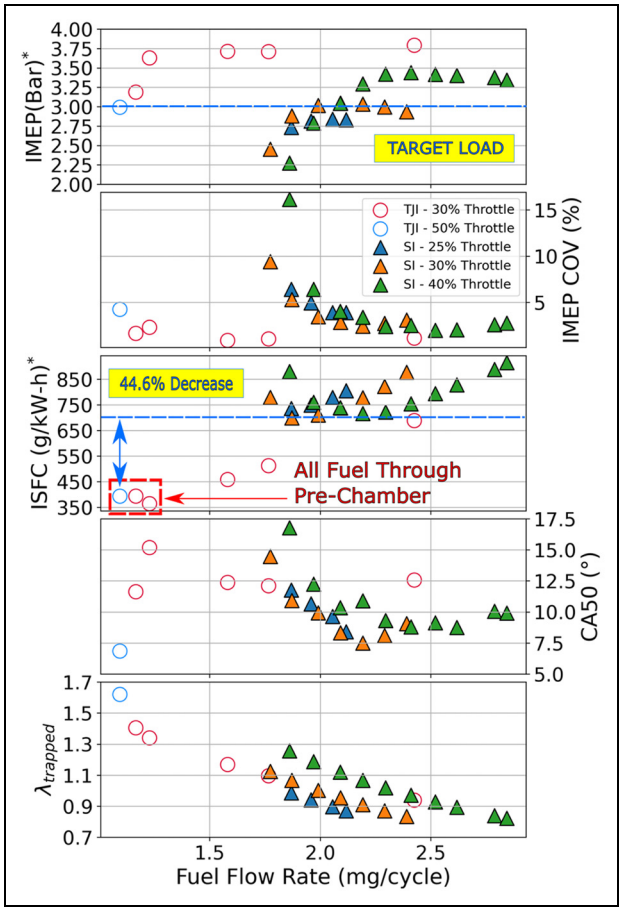

Figure 15. IMEP, COV, ISFC, CA50, and trapped lambda using CN50 fuel with 3000 rpm, 3 bar target.
*IMEP and ISFC corrected for pre-chamber parasitic loss.

performance under low-speed, low-throttle conditions, where main chamber scavenging is poor and passive TJI systems are likely to struggle due to insufficient pre-chamber scavenging.[28] At the cruising speed condition, the SFC of the SI system improved considerably with the improved main chamber scavenging, although the TJI system still achieved a 29.7% reduction in fuel consumption over SI at this operating point after accounting for the pre-chamber parasitic losses. Again, the trapped AFR result suggests the TJI system was operated slightly leaner than the SI system at the lowest SFC point for this fuel and operating condition.

Figure 17 shows the burn duration versus IMEP for gasoline and both kerosene-based fuels, where the data have been organized by the shortest burn duration within 0.2 bar intervals. Similar burn rates were observed across the fuels tested, and the TJI system exhibits a significantly shorter burn duration under both operating conditions. There appears to have been a slightly larger difference in burn duration at the 3000 rpm operating point across the load range. This result suggests the air-scavenged TJI system may be especially beneficial for maintaining good combustion performance under low speed, throttled conditions, where challenges associated with in-cylinder residuals have limited the adoption of passive pre-chambers on two-stroke architectures.[28]

Effect of pre-chamber air pressure

During the TJI experiments, the pre-chamber scavenge air pressure was adjusted up to 25 PSIg, where the results presented in the previous section isolated the lowest specific fuel consumption after accounting for the parasitic losses in alignment with equation (5). This section demonstrates the effect of varying the pre-chamber air pressure on engine performance and the minimum pressure requirements to achieve the target operating conditions while fueling only through the pre-chamber.

Figure 18 shows the IMEP, 10-90 burn duration, and pre-chamber air flow rate versus engine speed for each ignition mode using CN50 fuel. Several pre-chamber air pressure levels are presented for the TJI result. These experiments were conducted at wide-open throttle conditions, and the IMEP results for the TJI system have been corrected again to account for the parasitic pre-chamber scavenging work. The TJI system achieved a slight increase in load over SI across the operating range, where the highest scavenge air

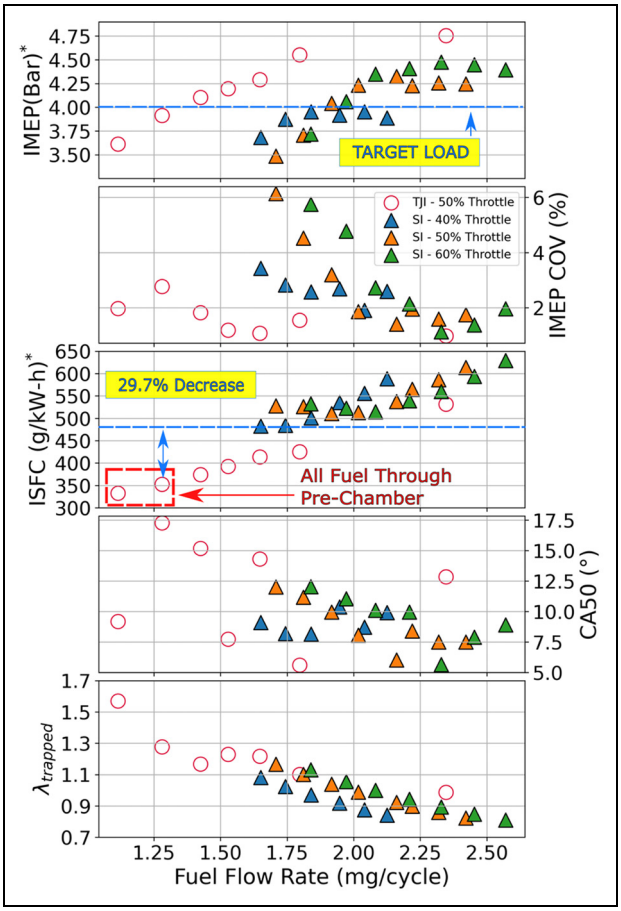

Figure 16. IMEP, COV, ISFC, CA50, and trapped lambda using CN50 fuel with 5000 rpm, 4 bar target.
*IMEP and ISFC corrected for pre-chamber parasitic loss.

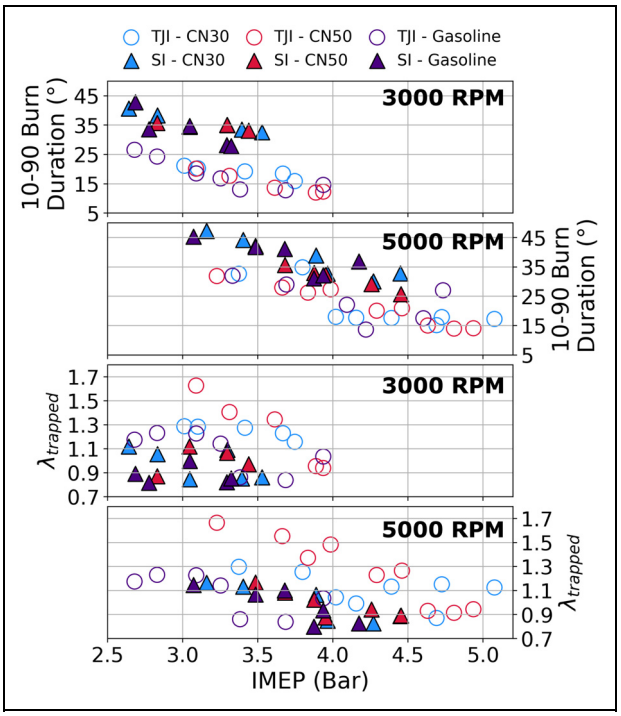

Figure 17. 10-90 burn duration and trapped lambda for gasoline, CN30, and CN50 kerosene-based fuels at 3000 and 5000 rpm.

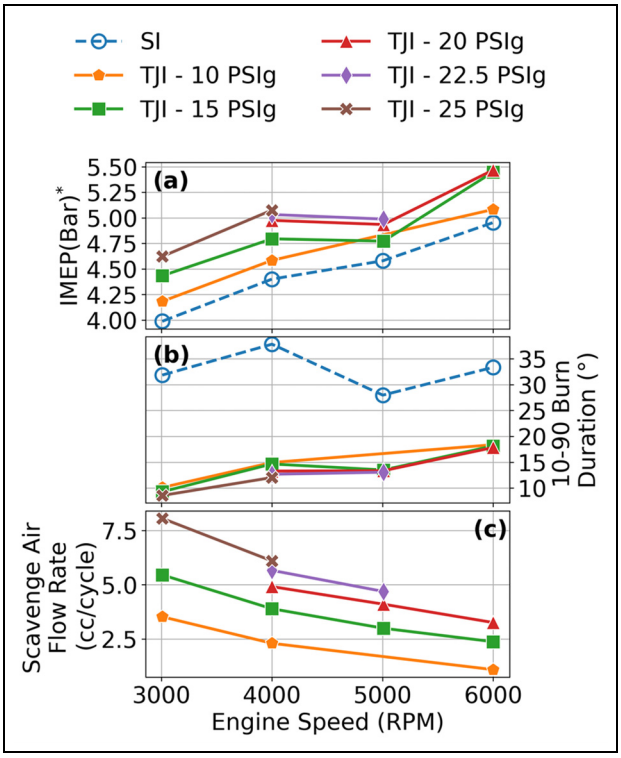

Figure 18. IMEP (a), 10-90 burn duration (b), and pre-chamber scavenge air flow rate (c) versus engine speed and pre-chamber air pressure at WOT using CN50 fuel.
*IMEP corrected for pre-chamber parasitic loss.

pressure yields the maximum load. The pre-chamber scavenge air has a slight supercharging effect; however, in practice, the air compressor would likely be sized for the lowest possible flow rate to minimize weight. The IMEP using the TJI system was 5%–15% higher than the SI system across the operating range, depending on the pre-chamber air pressure. The burn duration observed during this test was marginally dependent on the pre-chamber air pressure, although it was significantly faster for the TJI system for all operating conditions. The burn duration using the TJI system increased with engine speed, with a minimum of about 10° at 3000 rpm, and a maximum of about 18° at 6000 rpm. This trend in burn duration is likely influenced by the decreasing air flow on a per-cycle basis with increasing engine speed, as shown in Figure 18(c). At higher engine speeds, the poppet valve is open for a shorter time interval, requiring a higher scavenge air pressure to maintain the same air flow per cycle. There was no clear trend in burn duration versus RPM for the SI result, which was relatively constant from roughly 30° to 35°.

As discussed in the previous section, the fuel economy benefits of using Jetfire TJI ignition are maximized when the bulk fueling is entirely delivered through the pre-chamber, because this strategy minimizes fuel short-circuiting during main chamber scavenging. Therefore, the minimum air pressure requirement at the two target operating conditions was examined with all the fuel being delivered through the

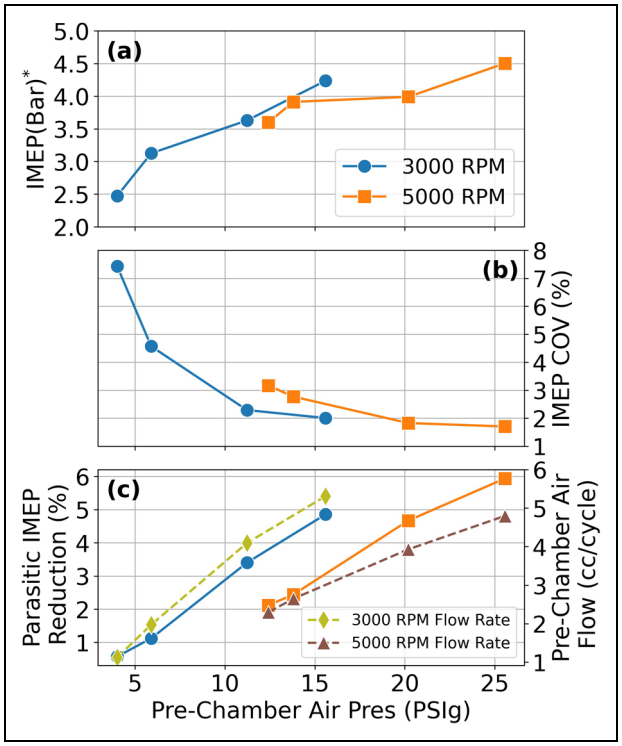

Figure 19. IMEP (a), COV (b), pre-chamber parasitic loss and air flow rate (c) versus pre-chamber air pressure using heavy fuel at 3000 and 5000 rpm. All fuel delivered through the pre-chamber.
*IMEP corrected for pre-chamber parasitic loss.

pre-chamber. Figure 19 presents IMEP and COV versus pre-chamber air pressure while fueling entirely through the pre-chamber with either CN30 or CN50 Fuel. The 3000 rpm, 3 bar target could be achieved with as little as 6 PSIg air pressure, which resulted in about a 1% parasitic IMEP loss (0.035 bar). Lower pre-chamber air pressure resulted in a sharp decrease in combustion stability and a corresponding decrease in load. It is worth noting that the TJI system can operate with little to no pre-chamber air, provided that bulk fueling is delivered via the main chamber crankcase injector, although this results in higher fuel consumption. The minimum air pressure required to achieve the 5000 rpm, 4 bar operating target with all fuel delivered via the pre-chamber was approximately 15 PSIg, resulting in a 3% reduction in the measured IMEP, or roughly a 0.12 bar loss. Extending the pre-chamber valve lift duration may reduce the air pressure requirement, but could also increase fuel short-circuiting if the valve opens during main chamber scavenging. Thus, optimizing the pre-chamber valve timing, valve duration, and injection timing would likely yield benefits concerning efficiency and parasitic losses.

Note that these estimates of parasitic losses were obtained under ambient conditions near atmospheric pressure. At altitude, a higher pressure would be required to maintain an equivalent mass flow rate, leading to higher parasitic losses. Assuming a simplified flow through an orifice, the required pressure differential to maintain a constant mass flow rate increases as air density decreases. Group 3 UAS systems are categorized by a nominal flight altitude up to 18,000 ft. At an altitude of 15,000 ft, the parasitic work required to deliver an equivalent mass of air per cycle increases by approximately 80% relative to at sea level. This suggests a parasitic MEP loss of approximately 5.5% at altitude if the scavenge air mass flow requirement were to remain equivalent to that under the experimental test conditions.

Conclusions and future work

This study examined an active pre-chamber ignition system with supplemental air scavenging for use in a small-bore two-stroke engine for drone applications. The engine was operated in both spark ignition (SI) and turbulent-jet ignition (TJI) modes using either gasoline or kerosene-based military fuels. Fuel was delivered via a crankcase injector for the SI experiments. For the TJI experiments, the crankcase fueling was reduced or eliminated, and much or all of the bulk charge was delivered through the pre-chamber injector. The main conclusions are summarized below.

- The air scavenged TJI system can operate reliably under moderate air pressure (6–15 PSIg), with the bulk charge being delivered only through the pre-chamber for low-speed and cruising conditions.
- When fueling only through the pre-chamber, the TJI system achieved a 37.3%–44.6% reduction in fuel consumption at the 3000 rpm and 3 bar indicated mean effective pressure (IMEP) operating condition, depending on the fuel used. At an approximate cruising condition (5000 rpm, 4 bar IMEP), the TJI system achieved a 28.5%–30.9% reduction in fuel consumption over SI for the various fuels examined.
- Exhaust O_2 measurements indicate 30%–45% of the fuel is short-circuited using the SI ignition mode under the studied operating conditions. These results suggest that the air-scavenged TJI system can significantly reduce the short-circuited fraction while simultaneously maintaining excellent combustion stability under low to moderate speeds and loads.
- When comparing the two ignition systems at their most optimal specific fuel consumption (SFC), the TJI ignition and fueling strategy exhibits up to 50% lower hydrocarbon emissions.
- The air-scavenged TJI system accelerated the burn rate by up to nominally 50% under both operating conditions examined in this work.

Limitations and future work

This study was limited to moderate-speed operating conditions due to the maximum speed limit of the dynamometer. It will be critical to evaluate the

performance of the Jetfire TJI system under high-speed, maximum power conditions, as this is another operating regime where passive pre-chambers have been shown to fall short of SI unless the geometry of the passive pre-chamber is optimized for high-speed operation.[27,28] It is believed that the active pre-chamber fueling system will resolve the issue of insufficient time for fuel transport through the pre-chamber orifices reported by other researchers. Performance of the pre-chamber poppet valve will also need to be assessed under these high-speed regimes. A rotary pre-chamber scavenge valve concept is under development for this system, which may reduce the valvetrain weight and offer superior valve performance at high engine speeds. The optimization of the pre-chamber valve timing and duration should also be assessed.

A comparison against LPDI would further isolate the benefits of the pre-chamber over the injection strategy. While a direct injection system would also significantly reduce fuel short circuiting, it is likely that the pre-chamber ignition strategy would still be advantageous for igniting highly stratified mixtures under late injection timing. Knock tolerance testing is currently underway, although the loads examined in the work described in this paper were not prone to knocking with the CN50 fuel. Finally, a three-cylinder variant of the TJI system with an integrated air compressor would enable a direct comparison of brake output and efficiency with a traditional SI system, thereby eliminating any assumptions regarding parasitic losses.

Acknowledgements

The authors thank Cobra Aero LLC for providing the two-stroke engine platform and technical support. The authors also wish to acknowledge Michigan State University for providing the test facility.

ORCID iD

Daniel Nicklowitz https://orcid.org/0009-0006-4388-8144

Funding

The authors received no financial support for the research, authorship, and/or publication of this article.

Declaration of conflicting interests

The authors declared the following potential conflicts of interest with respect to the research, authorship, and/or publication of this article: Dr. Harold Schock owns Jetfire Power LLC, which develops pre-chamber technologies investigated within this work. All other authors declare no competing interests.

References

1. Ishibashi Y and Asai M. A low pressure pneumatic direct injection two-stroke engine by activated radical combustion concept. *SAE Technical Paper* 980757, 1998. https://doi.org/10.4271/980757; https://www.sae.org/content/980757//
2. Ausserer JK, Horn K, Polanka M, et al. Quantification of short-circuiting and trapping efficiency in a small internal combustion engine by GC-MS and GC-TCD. *SAE Technical Paper* 2015-32-0716, 2015. https://doi.org/10.4271/2015-32-0716; https://www.sae.org/content/2015-32-0716
3. J Heywood (ed.). *Two-stroke cycle engine: its development, operation and design*. 1st ed. CRC Press LLC, 1999.
4. Badami M, Marzano MR, Millo F, et al. Comparison between direct and indirect fuel injection in an S.I. two-stroke engine. *SAE Technical Paper* 1999-01-3311, 1999. https://doi.org/10.4271/1999-01-3311; https://www.sae.org/content/1999-01-3311//
5. Romani L, Vichi G, Balduzzi F, et al. Fine-tuning of a two stoke engine in full power configuration provided with a low pressure direct injection system. *Energy Proc* 2017; 126: 987–994. pii: S1876610217337578. https://doi.org/10.1016/j.egypro.2017.08.251; https://linkinghub.elsevier.com
6. Dube A and Ramesh A. Influence of injection parameters on the performance and emissions of a direct injection two stroke SI engine. *SAE Technical Paper* 2016-01-1052, 2016. https://doi.org/10.4271/2016-01-1052; https://www.sae.org/content/2016-01-1052/
7. Sogawa M and Kato M. Development of the high pressure direct injection (HPDI) system for two-stroke outboard motor. *SAE Technical Paper* 2001-01-1786, 2001. https://doi.org/10.4271/2001-01-1786; https://www.sae.org/content/2001-01-1786/
8. Bertsch M, Beck KW, Matousek T, et al. Is a high pressure direct injection system a solution to reduce exhaust gas emissions in a small two-stroke engine? SAE paper, 2013. https://doi.org/10.4271/2013-32-9143; http://www.sae.org/technical/papers/2013-32-9143.
9. Worth D, Coplin N, McNiff M, et al. Design considerations for the application of air assisted direct in-cylinder injection systems. *SAE Technical Paper* 978452, 1997: 2688–3627. https://doi.org/10.4271/978452; https://www.sae.org/content/978452
10. Padala S, Bansal A and Ramesh A. Studies on an air assisted gasoline direct injection system for a two-stroke engine. *SAE Technical Paper* 2008-28-0048, 2008. https://doi.org/10.4271/2008-28-0048; https://www.sae.org/content/2008-28-0048/.
11. Cathcart G, Dickson G and Ahern S. The application of air-assist direct injection for spark-ignited heavy fuel 2-stroke and 4-stroke engines. *SAE paper*, 2005. https://doi.org/10.4271/2005-32-0065; http://www.crossref.org
12. Leighton S and Ahern S. Fuel economy advantages on Indian 2-stroke and 4-stroke motorcycles fitted with direct fuel injection. *SAE Technical Paper* 2003-26-0019, 2003. https://doi.org/10.4271/2003-26-0019; https://www.sae.org/content/2003-26-0019/
13. Hoogterp-Decker L and Schihl P. The use of synthetic JP-8 fuels in military engines. *Army Science Conference*, U.S. Army TARDEC, 2010.
14. Falkowski DT, Abata DL and Cho P. The performance of a spark-ignited stratified-charge two stroke engine operating on a kerosine based aviation fuel. *SAE Technical Paper* 972737, 1997. https://doi.org/10.4271/972737; https://www.sa e.org/content/972737/

15. Wang L, Zhao Z, Yu C, et al. Experimental study of aviation kerosene engine with PJI system. *Energy* 2022; 248: 123590. pii: S0360544222004935. https://doi.org/10.1016/j.energy.2022.123590; https://linkinghub.elsevier.com
16. Yu S and Zheng M. Future gasoline engine ignition: A review on advanced concepts. *Int J Engine Res* 2021; 22(6): 1743–1775. https://doi.org/10.1177/1468087420953085; https://journals.sagepub.com
17. Tian J, Xiong Y, Liu Z, et al. Experimental study on the discharge characteristics of high-voltage nanosecond pulsed discharges and its effect on the ignition and combustion processes. *Appl Energy* 2024; 374: 124011. pii: S0306261924013941. https://doi.org/10.1016/j.apenergy.2024.124011; https://linkinghub.elsevier.com
18. Tian J, Wang L, Xiong Y, et al. Enhancing combustion efficiency and reducing nitrogen oxide emissions from ammonia combustion: a comprehensive review. *Process Saf Environ Prot* 2024; 183: 514–543. https://doi.org/10.1016/j.psep.2024.01.020; pii: S0957582024000211; https://linkinghub.elsevier.com
19. Yang X, Wang P, Zhao Q, et al. Effect of spark timing on the pre-chamber jet ignition in a lean-burn natural gas engine. *Int J Engine Res* 2023; 24(8): 3556–3573. https://doi.org/10.1177/14680874231162919; https://journals.sagepub.com/doi/10.1177/14680874231162919
20. Trombley G, Toulson E, Kim K, et al. Passive turbulent jet ignition of jet fuel in a rapid compression machine. *Appl Therm Eng* 2024; 257: 124471. pii: S1359431124021392. https://doi.org/10.1016/j.applthermaleng.2024.124471; https://linkinghub.elsevier.com
21. Cui H, Zhao Z, Zhang F, et al. Effect of pre-chamber volume on combustion characteristics of an SI aircraft piston engine fueled with RP3. *Fuel* 2021; 286: 119238. pii: S0016236120322341. https://doi.org/10.1016/j.fuel.2020.119238; https://linkinghub.elsevier.com
22. Nicklowitz D, Stuecken T, Schock H, et al. Evaluation of jetfire pre-chamber ignition for lean, DI homogeneous charge, heavy fueled combustion and multi-fuel capability. *SAE Technical Paper* 2024-01-4134, 2024. https://doi.org/10.4271/2024-01-4134; https://www.sae.org/content/2024-01-4134
23. Hu C, Zhang Z, Tian M, et al. Research on application of asymmetrical pre-chamber in air-assisted direct injection kerosene engine. *Appl Therm Eng* 2022; 204: 117919. pii: S1359431121013417. https://doi.org/10.1016/j.applthermaleng.2021.117919; https://linkinghub.elsevier.com
24. Liu F, Zhou L, Hua J, et al. Effects of pre-chamber jet ignition on knock and combustion characteristics in a spark ignition engine fueled with kerosene. *Fuel* 2021; 293: 120278. pii: S001623612100154X. https://doi.org/10.1016/j.fuel.2021.120278; https://linkinghub.elsevier.com
25. Attard WP, Blaxill H, Anderson EK, et al. Knock limit extension with a gasoline fueled pre-chamber jet igniter in a modern vehicle powertrain. *SAE Int J Engines* 2012; 05(3): 1201–1215. https://doi.org/10.4271/2012-01-1143; https://www.sae.org/content/2012-01-1143/
26. Rajasegar R, Srna A, Novella R, et al. Exploring the EGR dilution limits of a pre-chamber ignited heavy-duty natural gas engine operated at stoichiometric conditions - an optical study. *SAE paper 2023-01-0256*, 2023. https://doi.org/10.4271/2023-01-0256; https://www.sae.org/content/2023-01-0256
27. Bosi L, Ciampolini M, Romani L, et al. Experimental analysis on the effects of passive prechambers on a small 2-stroke low-pressure direct injection (LPDI) engine. *SAE Technical Paper* 2020-32-2305, 2020. https://doi.org/10.4271/2020-32-2305; https://www.sae.org/content/2020-32-2305/
28. Bosi L, Ciampolini M, Raspanti S, et al. Jet ignition in small two-stroke engines: an experimental survey on benefits and challenges. In: *Proceedings of the E3S web of conferences*, 2021, Vol. 312, p. 07012. EDP Sciences. https://doi.org/10.1051/e3sconf/202131207012; https://www.e3s-conferences.org/10.1051/e3sconf/202131207012
29. Atis CAA, Ayele Y, Stuecken T, et al. Effect of prechamber scavenging strategy on EGR tolerance and thermal efficiency of pre-chamber turbulent jet ignition systems. *Int J Engine Res* 2023; 24(5): 1938–1960. https://doi.org/10.1177/14680874221105162; http://journals.sagepub.com
30. Atis C and Schock H. Comparison of excess air (lean) vs EGR diluted operation in a pre-chamber air/fuel scavenged dual mode, turbulent jet ignition engine at high dilution rate (~40%) *SAE Int J Adv Curr Pract Mobil* 2021; 03(4): 1569–1584. https://doi.org/10.4271/2021-01-0455; https://www.sae.org/content/2021-01-0455
31. Atis C, Chowdhury SS, Ayele Y, et al. Ultra-lean and high EGR operation of dual mode, turbulent jet ignition (DM-TJI) engine with active pre-chamber scavenging. *SAE paper 2020-01-1117*, 2020. https://doi.org/10.4271/2020-01-1117; https://www.sae.org/content/2020-01-1117/
32. Tolou S and Schock H. Experiments and modeling of a dual-mode, turbulent jet ignition engine. *Int J Engine Res* 2020; 21(6): 966–986. https://doi.org/10.1177/1468087419875880; https://journals.sagepub.com
33. Vedula RT, Song R, Stuecken T, et al. Thermal efficiency of a dual-mode turbulent jet ignition engine under lean and near-stoichiometric operation. *Int J Engine Res* 2017; 18(10): 1055–1066. https://doi.org/10.1177/1468087417699979; https://journals.sagepub.com
34. Cobra AERO LLC. Cobra Aero A99HF Data Sheet. Cobra AERO LLC, https://static1.squarespace.com/static/5d895cd1d064367698a1205a/t/681cd92f742b4365f20e4cdd/1746721072818/A99HF_data_sheet.pdf (2025, accessed 10 July 2025).
35. Jackson R. *Three-pot power*. Unscrewed Systems Technology, 2022. ps://static1.squarespace.com/static/5d895cd1d064367698a1205a/t/62ceca1999543b6b3b8ec75f/1657719322042/Uncrewed + Systems + Technology + 044 + 1 + Cobra + AERO + A99N.pdf
36. MJ Moran (ed.). *Fundamentals of engineering thermodynamics*. 8th ed. Wiley, 2014.
37. JB Heywood (ed.). *Internal combustion engine fundamentals*. 2nd ed. McGraw-Hill Education, 2018.
38. Enigneering ToolBox. Gasoline - Density, Specific Heat, Viscosity and Thermal Conductivity vs. Temperature. *Engineering ToolBox*. https://www.engineeringtoolbox.com/gasoline-density-specific-heat-dynamic-kinematic-viscosity-thermal-conductivity-vs-temperature-d_2224.html (n.d., accessed 29 December 2025).
39. Enigneering ToolBox. Flash Points - Liquids. *Engineering ToolBox*. https://www.engineeringtoolbox.com/flash-point-fuels-d_937.html (n.d., accessed 13 April 2026).
40. Douglas R. AFR and emissions calculations for two-stroke cycle engines. *SAE Trans* 1990; 99: 1909–1920. https://www.jstor.org/stable/44548201